Entanglement entropy of spherical domains in anti-de Sitter space

Pavel Krtouš*

ITP, Faculty of Mathematics and Physics, Charles University in Prague, V Holešovičkách 2, Prague, Czech Republic

Andrei Zelnikov†

TPI, Department of Physics, University of Alberta, Edmonton, Alberta T6G 2E1, Canada

(Dated: November 7, 2013)

It was proposed by Ryu and Takayanagi that the entanglement entropy in conformal field theory (CFT) is related through AdS/CFT correspondence to the area of a minimal surface in the bulk. We apply this holographic geometrical method of calculation of the entanglement entropy to study the vacuum case of CFT which is holographically dual to empty anti-de Sitter (AdS) spacetime. We present all possible minimal surfaces spanned on one or two spherical boundaries at AdS infinity. We give exact analytical expressions for regularized areas of these surfaces and identify finite renormalized quantities. In the case of two disjoint boundaries the existence of two nontrivial phases is confirmed, as well as the discontinuous character of the phase transition to the trivial phase. The exact analytical results are thus consistent with previous numerical and approximative computations. We also briefly discuss the character of a spacetime extension of the minimal surface spanned on two uniformly accelerated boundaries.

PACS numbers: 03.65.Ud, 11.25.Tq, 04.60.-m

INTRODUCTION

The famous Bekenstein–Hawking area law [1, 2]

$$S_{BH} = \frac{k_B c^3}{\hbar}\frac{A}{4\,G} \tag{1}$$

for the entropy of black holes connects thermodynamics, gravity and relativistic quantum field theory. This relation remains valid not only for the Einstein gravity in four dimensions but in higher dimensions too, as soon as the gravitational constant G is the D-dimensional one and the area A is understood as the volume of $(D-2)$-dimensional surface of the horizon.

If quantum field theory (QFT) is defined on the manifold with a boundary an entanglement entropy is known to have a very similar dependence on the area of the boundary [3, 4]. This analogy with the black hole entropy is not accidental. If one considers black hole horizon as the surface separating the interior of the black hole from its exterior, then the corresponding entanglement entropy reduces to the Bekenstein–Hawking entropy [5]. Quantum fields on a curved background spacetime also lead to the renormalization of the effective gravitational constant. It's amazing that quantum corrections to the entropy per unit area of a horizon are equivalent to the quantum corrections to the gravitational coupling [6]. The interpretation of the Bekenstein–Hawking formula as an entanglement entropy becomes even more striking in the framework of induced gravity models [7–11]. It was proposed in [5], that in generic static spacetimes with horizons, the the minimal area surface on the $t = \text{const}$ slice of the spacetime may play an important role in defining the entanglement entropy of the black hole.

Recently, holographic computations of the entanglement entropy in conformal field theory (CFT) at infinity of Anti-de Sitter (AdS) spacetime got a lot of attention and developments. The original conjecture for entanglement entropy by Ryu and Takayanagi [12–14] is that in a static configuration the entanglement entropy of a subsystem localized in a domain Ω is given by the formula[1]

$$S_\Omega = \frac{A_{\Sigma_\Omega}}{4\,G}. \tag{2}$$

Given a static time slice (the $(D-1)$-dimensional bulk space), the $(D-2)$-dimensional domain Ω belongs to infinite boundary $\mathcal{I}$ of the bulk and the area A_{Σ_Ω} in Eq. (2) is to be understood as the area of a $(D-2)$-dimensional minimal surface Σ_Ω in the bulk spanned on the boundary $\partial\Omega$ of the subsystem (i.e., $\partial\Sigma_\Omega = \partial\Omega$).

The QFT derivation of the Ryu–Takayanagi formula was given by Fursaev [15] using the replica trick. In QFT with gravity duals the formula (2) was proven for AdS_3 [16, 17]. In a more general case of Euclidean gravity solutions without Killing vectors the arguments supporting a validity of Ryu-Takayanagi formula were given in [18, 19]. In the last few years the conjecture by Ryu and Takayanagi has been generalized to gravity theories with higher curvature interactions [20–23] or some other deformations of the gravity theory [24]. The excellent up-to-date review of the entanglement entropy and black holes one can find in [25].

The computation of an entanglement entropy for subsystem localized in two disjoint regions is particularly

* Pavel.Krtous@utf.mff.cuni.cz

† zelnikov@ualberta.ca

[1] From now on we use $k_B = c = \hbar = 1$ system of units.

interesting, since it can be used as a probe of the confinement [26, 27]. It was demonstrated [26, 28] that in confining backgrounds there are generally more solutions for minimal surfaces in the bulk spanned on the boundaries of these disjoint regions. However, there is a maximum distance between the regions for which the tube-like minimal surface connecting both components ceases to exist. There is also a critical scale when disconnected minimal surfaces solution dominates over the connected one. In the QFT language this critical behavior is analogous to finite temperature deconfinement transition.

In the case of a few disjoint regions the minimal surfaces connecting their boundaries are generally not unique and their areas differ. The conventional wisdom is that the entanglement entropy is related with the surfaces with the least area. This choice guarantees the required strong subadditivity property [29] of the entanglement entropy. There were some proposals [30] how to modify this "least area" rule while still satisfying the strong subadditivity property.

In this paper we study minimal surfaces in pure AdS spacetime. We show that many properties of the entanglement entropy, like critical behavior [26] demonstrated for the asymptotically AdS spacetimes with a black holes in the bulk, exist already in the pure AdS. The main result is that we are able to find exact solutions for all minimal surfaces spanned on one or two spherical boundaries arbitrary positioned at conformal infinity $\mathcal{I}$. In this short paper we give analytical formulas for the regularized and renormalized area of these minimal surfaces. The explicit form of the surfaces and its derivation is presented in more detailed paper [31]. We also shortly discuss spacetime character of a minimal surface spanned on two accelerated spherical domains.

SPHERICAL BOUNDARIES AT INFINITY

We start with geometrical preliminaries concerning the bulk space and with the characterization of the spherical domains at infinity. We will discuss only 3+1-dimensional AdS spacetime, although, the most of the discussion can be extended to higher dimensions.

AdS spacetime has many Killing symmetries and can be viewed as a static spacetime in various ways. However, in all cases the spatial section—the bulk space—has the hyperbolic geometry of Lobachevsky space. To describe it, we use cylindrical coordinates ρ, ζ, φ and Poincaré coordinates $\bar{x}$, $\bar{y}$, $\bar{z}$ in which the metric reads

$$\frac{1}{\ell^2}\,\boldsymbol{g}_{\text{Lob}}=\boldsymbol{d}\rho^2+\operatorname{ch}^2\!\rho\,\boldsymbol{d}\zeta^2+\operatorname{sh}^2\!\rho\,\boldsymbol{d}\varphi^2=\frac{1}{\bar{z}^2}\left(\boldsymbol{d}\bar{x}^2+\boldsymbol{d}\bar{y}^2+\boldsymbol{d}\bar{z}^2\right). \tag{3}$$

Here, ℓ is the characteristic scale describing the radius of curvature of AdS, as well as of its spatial section. The coordinates are related by $\bar{z}=\bar{r}/\operatorname{ch}\rho$, $\bar{x}=\bar{r}\operatorname{th}\rho\cos\varphi$, $\bar{y}=\bar{r}\operatorname{th}\rho\sin\varphi$, with $\bar{r}=\exp\zeta$.

The conformal infinity $\mathcal{I}$ of the spatial section is conformal sphere. In cylindrical coordinates it is given by $\rho\to\infty$ or $\zeta\to\pm\infty$. In Poincaré coordinates it is represented by plane $\bar{z}=0$ plus one improper point $\bar{r}\to\infty$.

By the *circular* (in higher dimension, *spherical*) boundary $\partial\Omega$ of a ball-like domain Ω at infinity $\mathcal{I}$ we mean a 1-dimensional surface given by infinite points of a 2-dimensional hyperplane in the bulk (hyperplane in the sense of hyperbolic geometry). The circular boundaries at infinity are thus in one-to-one correspondence with hyperplanes in the bulk. The boundary $\partial\Omega$ can be understood also as the boundary of the complementary domain $\mathcal{I}\backslash\Omega$.

From a point of view of the conformally spherical geometry on $\mathcal{I}$, all such boundaries are equivalent. It is a reflection of the trivial fact that all hyperplanes in the bulk are isometric. Therefore we do not have any quantity measuring a 'size' of spherical boundaries at infinity.

However, in many calculations, both in the bulk or at infinity, we need to regularize various quantities. Instead of working at $\mathcal{I}$ we restrict on some cut-off surface which is almost at infinity. Then we can measure a size of the circular boundaries using geometry on the cut-off surface. But, since the choice of the cut-off can be rather arbitrary, the regularized size of the spherical boundary can be only an intermediate quantity and physically measurable quantities should be cut-off independent.

Two circular boundaries can be in three qualitatively distinct positions: (i) disjoint boundaries (corresponding hyperplanes are ultraparallel), [2] (ii) boundaries crossing each other (the hyperplanes intersect in a line), and (iii) boundaries touching in one point (the corresponding hyperplanes are asymptotic).

In the first case we can define the distance of the boundaries as a distance of the corresponding hyperplanes. To the crossing circular boundaries we can assign an angle of the corresponding hyperplanes. Finally, all pairs of touching boundaries are equivalent. Indeed, all pairs of asymptotic hyperplanes in an arbitrary position are isometric to each other. In global hyperbolic space there is no measure which could distinguish them.

SURFACE SPANNED ON ONE BOUNDARY

Now we remind known results for a minimal surface spanned on one circular boundary. Such a minimal surface is trivial: it is the hyperplane which defines the boundary. If we choose the axis of the cylindrical coordinates perpendicular to the hyperplane, the hyperplane is given by $\zeta=\text{const}$. For the axis inside the hyperplane, the hyperplane is given by $\varphi=\varphi_0,\ \varphi_0+\pi$. In the Poincaré coordinates the hyperplane is represented as a plane orthogonal to the infinity surface $z=0$ or as

---

[2] Let us note that two circles positioned 'side by side' or 'one inside of another' in Poincaré planar representation of infinity are equivalent; they differ only by a choice of the improper point which closes planar part of infinity into sphere.

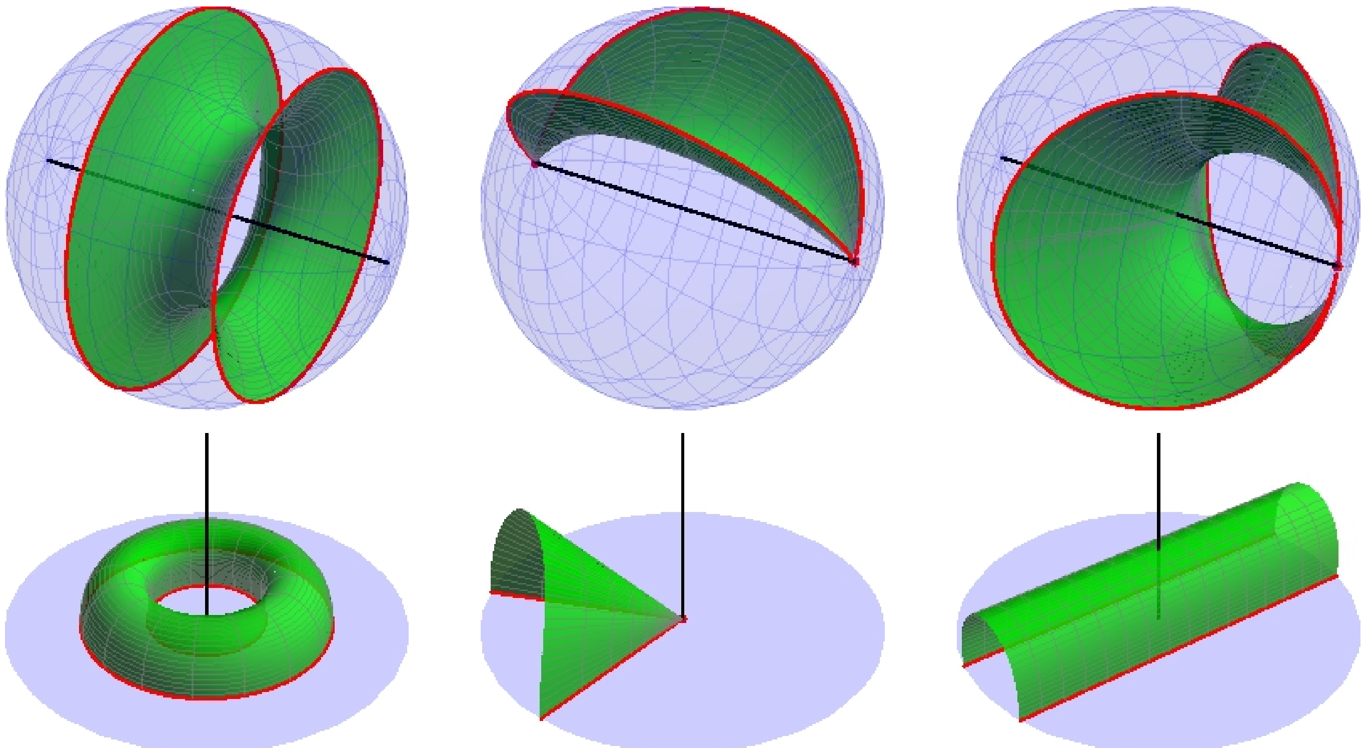

Figure 1. **Minimal surfaces spanned on circular boundaries.** The surfaces are visualized in Poincaré spherical (top) and Poincaré half-space (bottom) models. (a) The tube-like surface spanned on two disjoint boundaries. (b) The surface spanned on two semicircles joining the opposite poles. (c) The surfaces spanned on two touching circles.

a hemisphere with the center at $z=0$ (here we used a language of the conformally related Euclidian geometry with Cartesian coordinates $\bar{x}$, $\bar{y}$, $\bar{z}$).

To demonstrate different regularizations used later, we can write down the area of a hyperplane measured up to cut-off. For the hyperplane othogonal to the axis we have

$$A_{\mathrm{hp}} = 2\pi\ell^2\left(\sqrt{1+P^2}-1\right) = C\ell\Big[1-\frac{1}{P}+\mathcal{O}\Big(\frac{1}{P^2}\Big)\Big] \ , \quad (4)$$

where $C = 2\pi\ell P$, with $P = \operatorname{sh}\rho_*$, is the circumference of the circular boundary on the cut-off surface $\rho = \rho_* \gg 1$.

For the hyperplane which includes the axis we have

$$A_{\mathrm{hp}} = 2L\,\ell\sqrt{1-Z^{-2}} = 2L\ell\Big[1+\mathcal{O}\Big(\frac{1}{Z^2}\Big)\Big] \ , \quad (5)$$

where $L = Z\Delta\zeta_*\ell$, with $Z = \operatorname{ch}\rho_*$, is the length of the boundary at the cut-off surface. In this case, the circular boundary is represented by two lines $\rho=\infty$, $\varphi = \text{const}$, $\zeta\in\mathbb{R}$. We thus have to introduce two cut-offs: ultraviolet one, $\rho = \rho_*$, in the direction away from the axis, and infrared[3] one, $\zeta = \pm\Delta\zeta_*/2$, along the axis.

[3] The distinction between ultraviolet (UV) and infrared (IR) cut-off is moreless conventional here. The cut-off labeling the regularized surface near infinity is called UV since it corrresponds to UV cut-off in related CFT. IR cut-off is extensive one, it corresponds to the length along a translation symmetry.

Finally, the area of the hyperplane represented by a half-plane in the Poincaré coordinates, say $\bar{x} = \text{const}$, is

$$A_{\mathrm{hp}} = L\ell \ . \quad (6)$$

$L = \Delta\bar{y}_*/\bar{z}_*$ is again the length of the circular boundary at the cut-off surface $\bar{z} = \bar{z}_* \ll 1$. It is also infrared divergent: one has to cut-off $\bar{y}$ direction at $\bar{y} = \pm\Delta\bar{y}_*/2$.

In all three cases we recognize well-known property that the leading diverging term of the minimal surface is (up to a constant scale) given by the regularized size of the boundary at infinity. Clearly, the exact expression for the divergent term depends on the regularization scheme, however, in all cases it can be interpreted as regularized size of the boundary at infinity [28, 32, 33].

The area of the trivial minimal surface spanned on one circular boundary can be used to eliminate infinite contributions to area for more complicated surfaces. We define the renormalized area of a surface by subtracting the area of hyperplanes spanned on the same boundaries at infinity. In this sense, the trivial minimal surface has vanishing renormalized area.

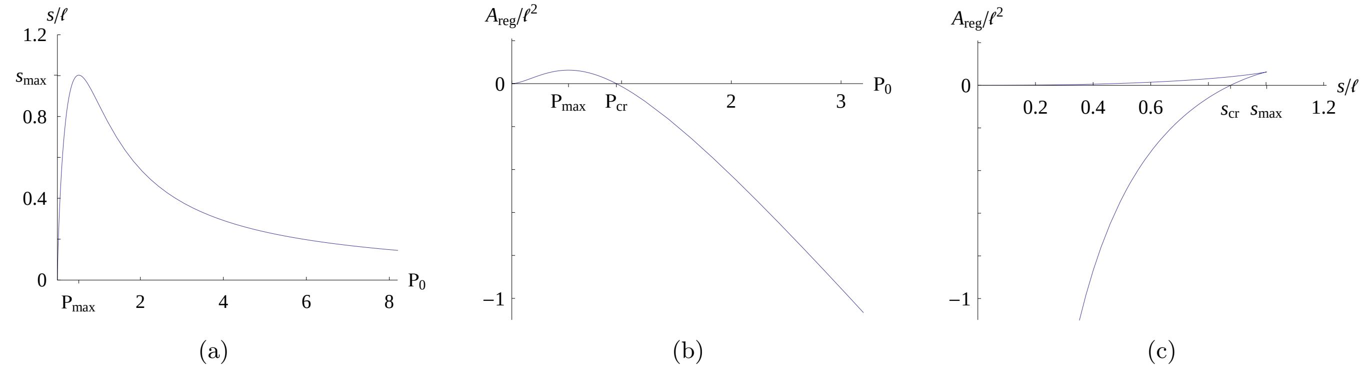

Figure 2. **Renormalized area of the minimal surface spanned on two boundaries.** (a) Relation between the distance s of the boundaries and the closest approach P_0 of the tube to the axis. (b) Renormalized area of the tube as a function of P_0. (c) Renormalized area as a function of the distance s.

SURFACES SPANNED ON TWO BOUNDARIES

Disjoint boundaries. Given two circular boundaries at infinity, we can always find the unique line perpendicular to the corresponding hyperplanes in the bulk. If we adjust the cylindrical coordinates to this axis, the circular boundaries are represented by two circles $\rho = \infty$, $\zeta = \pm\zeta_\infty$. It is possible to find [31] a tube-like minimal surface joining these two boundaries, see Fig. 1a. It is described by the function $\zeta(P)$ with $P = \operatorname{ch}\rho$ and it is parametrized by $P_0 = \operatorname{ch}\rho_0$ where ρ_0 is the closest approach of the surface to the axis:[4]

$$\begin{aligned}\zeta(P)=&\frac{\pm P_0}{\sqrt{1+P_0^2}\sqrt{1+2P_0^2}}\Big[(1+P_0^2)\,\mathsf{F}\Big(\arccos\tfrac{P_0}{P},\sqrt{\tfrac{1+P_0^2}{1+2P_0^2}}\Big)\\&-P_0^2\,\Pi\Big(\arccos\tfrac{P_0}{P},\tfrac{1}{1+P_0^2},\sqrt{\tfrac{1+P_0^2}{1+2P_0^2}}\Big)\Big]\,. \qquad (7)\end{aligned}$$

Setting $P = \infty$ we can read out the coordinates $\pm\zeta_\infty$ of the circular boundaries:

$$\begin{aligned}\zeta_\infty(P_0) =& \frac{P_0}{\sqrt{1+P_0^2}\sqrt{1+2P_0^2}}\\&\times\Big[(1+P_0^2)\,\mathsf{K}\Big(\sqrt{\tfrac{1+P_0^2}{1+2P_0^2}}\Big)-P_0^2\,\Pi\Big(\tfrac{1}{1+P_0^2},\sqrt{\tfrac{1+P_0^2}{1+2P_0^2}}\Big)\Big]\,. \qquad (8)\end{aligned}$$

The distance between both boundaries $s = 2\ell\zeta_\infty$ as a function of the parameter P_0 is depicted in Fig. 2a. It reveals that the tube exists only for distances smaller than the maximal distance $s_{\max} \approx 1.00229\ell$ and for these small distances there actually exist two tube-like minimal surfaces. One shallow one, remaining at large distances from the axis, and a deep one, approaching the axis. If the distance of circular boundaries is enlarged, the tube tears off and the minimal surface discontinuously splits into two trivial hyperplanes spanned on both boundaries.

To estimate which surface is the smallest one, we have to write down the regularized area:

$$\begin{aligned}A(P) =& \frac{4\pi\ell^2P_0^2}{\sqrt{1+2P_0^2}}\,\Pi\Big(\arccos\tfrac{P_0}{P},1,\sqrt{\tfrac{1+P_0^2}{1+2P_0^2}}\Big)\\=&\,2A_{\rm hp}+A_{\rm ren}+\mathcal{O}\Big(\frac{1}{P^3}\Big)\,. \qquad (9)\end{aligned}$$

The divergent term $A_{\rm hp}$ is given by (4), the finite part $A_{\rm ren}$ reads

$$\frac{A_{\rm ren}}{4\pi\ell^2} = 1+\frac{P_0^2}{\sqrt{1+2P_0^2}}\,\mathsf{K}\Big(\sqrt{\tfrac{1+P_0^2}{1+2P_0^2}}\Big)-\sqrt{1+2P_0^2}\,\mathsf{E}\Big(\sqrt{\tfrac{1+P_0^2}{1+2P_0^2}}\Big)\,. \qquad (10)$$

The renormalized area as a function of P_0 or of the distance s is shown in Fig. 2. We see that the shallow tube has always smaller area than the deeper one. However, for $s_{\rm cr} < s < s_{\max}$, the renormalized area of the tube is positive, i.e., the tube has larger area than the trivial solutions of two hyperplanes. The tube is thus the smallest minimal surface only for $s < s_{\rm cr} \approx 0.876895\ell$.

All these results are consistent with the previous numerical and approximate analysis [28].

Crossing circular boundaries. In the case of two crossing circular boundaries at infinity we naturally adjust the cylindrical coordinates to the axis going through the intersection points. Thus, the semicircles between these intersection points are represented by lines $\rho = \infty$, $\varphi = \text{const}$. In Poincaré coordinates they are half-lines in the plane $\bar z = 0$ starting at $\bar r = 0$. The minimal surface spanned on two such semicircles is depicted in Fig. 1b. Its explicit form can be found in [31]. It exists for any angle ϕ between both semicircles and can be parametrized by $Z_0 = \operatorname{ch}\rho_0$ with ρ_0 corresponding to the closest approach of the surface to the axis. The relation between of ϕ and Z_0 is one-to-one [31]. The regularized area takes form:

$$\begin{aligned}A(Z) =& \frac{2L\ell\,Z_0^2}{Z\sqrt{2Z_0^2-1}}\,\Pi\Big(\arccos\tfrac{Z_0}{Z},1,\sqrt{\tfrac{Z_0^2-1}{2Z_0^2-1}}\Big)\\=&\,A_{\rm hp}+\Delta\zeta_*\ell\Big[a_{\rm ren}+\mathcal{O}\Big(\frac{1}{Z^3}\Big)\Big]\,. \qquad (11)\end{aligned}$$

---

[4] The solutions are expressed in terms of eliptic integrals with a convention of [34].

The leading term $A_{\rm hp}$ is given by (5). It is divergent because both UV and IR divergencies. The next term is proportional to IR cut-off $\Delta\zeta_*$. The reason is that the minimal surface is invariant under the translation along the axis. However, we can write down the finite renormalized area density $a_{\rm ren} = \frac{A_{\rm ren}}{\Delta\zeta_*\ell}$:

$$a_{\rm ren}=2\ell\Big[\frac{Z_0^2}{\sqrt{2Z_0^2-1}}\,\mathsf{K}\Big(\sqrt{\tfrac{Z_0^2-1}{2Z_0^2-1}}\Big)-\sqrt{2Z_0^2-1}\,\mathsf{E}\Big(\sqrt{\tfrac{Z_0^2-1}{2Z_0^2-1}}\Big)\Big]\,. \tag{12}$$

It is always negative. Naturally, the surface has always smaller area then two half-hyperplanes starting at the axis reaching the semi-circles at infinity.

Touching circular boundaries Tangent circular boundaries are trivially represented in Poincaré coordinates. If oriented in $\bar{y}$ direction, they are given by $\bar{z}=0$, $\bar{x}=\pm\bar{x}_\infty$. The minimal surface spanned on such a 'strip' is in Fig. 1c, [31, 35]. It reaches the maximal value of the coordinate $\bar{z}$ for $\bar{z}_0=\bar{x}_\infty/X_0$, which we call the 'top-line' of the surface. The constant X_0 is given by $X_0=\frac{\Gamma(3/4)^2}{\sqrt{2\pi}}\approx 0.59907$. The area regularized at $\bar{z}\ll 1$ is

$$\begin{aligned} A(\bar{z}) = \frac{2\mathcal{A}\ell^2}{\bar{z}_0}\Bigg[&\sqrt{\frac{\bar{z}_0^2}{\bar{z}^2}-\frac{\bar{z}^2}{\bar{z}_0^2}}-\sqrt{2}\,\mathsf{E}\Big(\arccos\frac{\bar{z}}{\bar{z}_0},\frac{1}{\sqrt{2}}\Big)\\ &+\frac{1}{\sqrt{2}}\,\mathsf{F}\Big(\arccos\frac{\bar{z}}{\bar{z}_0},\frac{1}{\sqrt{2}}\Big)\Bigg]\\ = A_{\rm hp} + L_0\big[-2X_0\ell + O(\bar{z}^3)\big]\,. \end{aligned} \tag{13}$$

The leading divergent term $A_{\rm hp}$ is given by (6). The next term is IR divergent since the surface has the horocyclic symmetry $\bar{y}\to\bar{y}+\bar{y}_s$. It is thus proportional to the length $L_0=\frac{\Delta\bar{y}_*\ell}{\bar{z}_0}$ measured on the 'top-line' of the surface. The renormalized area density $a_{\rm ren}=\frac{A_{\rm ren}}{L_0}=-2X_0\ell$ is, as expected, a constant independent of the position of the touching circular boundaries.

DISCUSSION

Returning to the conjecture (2), we can now associate the entanglement entropy for any two generally positioned spherical domains at infinity. The most interesting case occurs for two disjoint domains. For the boundaries closer than $s_{\rm max}$ there are three possible minimal surfaces, which indicates that the corresponding system in CFT can be in three various phases. The physical one would be that with the smallest area. Inspecting Fig. 2b, one can see that the phase transition occurs at the distance $s=s_{\rm cr}$, when the area of the tube-like surface starts to exceed the area of the trivial solution of two hyperplanes. Although the entanglement entropy changes continuously with the distance between the boundaries at $s=s_{\rm cr}$, the corresponding minimal surface changes discontinuously.

To move from the trivial phase to tube-like phase continuously, one would have to start with two very close hyperplanes. At a point, where they almost touch, a very deep tube-like surface can appear. By enlarging the distance of the boundaries, the tube starts to grow wider. It follows the upper branch of the curve in Fig. 2c (i.e. the non-physical phase) till the maximal possible distance $s_{\rm max}$ of the boundaries. Here, one has to start decreasing the distance of the boundaries in such a way that the tube grows even wider (following the lower branch in Fig. 2c). After decreasing the distance under $s_{\rm cr}$ one obtains, in the continuous way, the physical tube-like phase.

The fact that the tube-like minimal surface does not exist for too distant boundaries can be explored also in a dynamical way. We consider a static Killing vector orbits of which have the acceleration larger than $1/\ell$. This Killing vector has a bifurcation character similar to the boost Killing vector in Minkowski spacetime. Its Killing horizons divide AdS space into pairs of static regions positioned acausally with respect to each other, with nonstatic regions between, cf. Fig. 3a. The hyperbolic space in which we found the tube-like solution is the spatial section of both opposite static regions. We can position one circular boundary at infinity of one static region and other one at infinity of opposite static region. The world-sheets of corresponding hyperplanes describe uniformly accelerated motion along the Killing vector, see Fig. 3a. The tube-like minimal surface can be also evolved into both static regions. However, it does reach the Killing

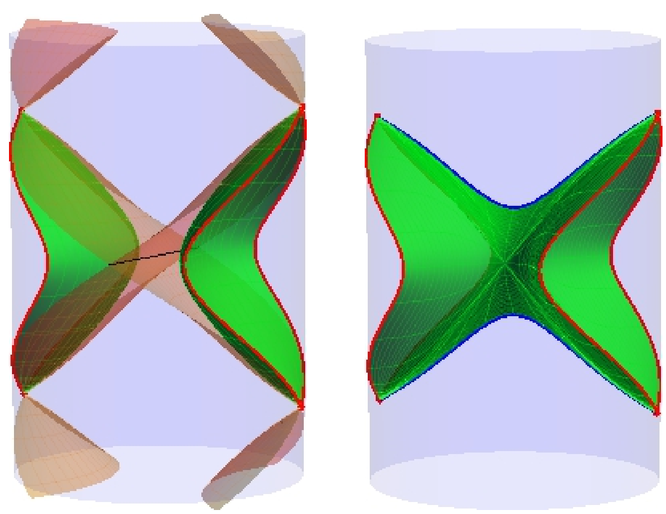

(a) (b)

Figure 3. **World-sheets of minimal surfaces.** Vertical cylinder represents 3+1 dimensional AdS spacetime with angular direction φ suppressed. The world-sheet of one circular boundary is thus reduced only to two curves at infinity. One circular boundary is localized in the left static region, other in the right one. (a) Two uniformly accelerated hyperplanes spanned on these circular boundaries. Killing horizons are indicated. (b) The world-sheet of the tube-like minimal surface joining the same circular boundaries.

horizons and there it must be extended into non-static regions. The resulting surface is depicted in Fig. 3b.

We see that the surface is non-smooth along two spatial edges, one describing the formation of the surface in the past, other its termination in the future. If the surface is viewed from the point of a globally static observer (the vertical direction in the figure), the future edge can be interpret as tearing off the surface for the boundaries positioned too far from each other and subsequent motion of the teared pieces. For more details see [31].

Beside the case of two spherical domains we can investigate even more complicated situations: let us consider spherical domains Ω_i, each of them being a subdomain of all following: $\Omega_i \subset \Omega_j$ for $i < j$. They do not have to be all simultaneously concentric! The circular boundaries of these domains correspond to ultraparallel hyperplanes in the bulk. For such a configuration we know minimal surfaces for any pair of the boundaries. Employing (2) we find that the renormalized entropy depends only on the distance of the boundaries, cf. (8), (9). We can thus test entropy properties for domains obtained by a combination of several subdomains. Namely, one can check the strong subadditivity inequalities to find that they are satisfied, as expected from general considerations [28].

Similarly one can study the systems of strips between several semicircles joined at the same poles.

We have found exact analytical solutions for minimal surfaces in AdS spacetime for two disjoint domains at its infinity. These classical geometrical solutions reveal the existence of different phases that reflect the phase transition in the corresponding quantum CFT, similar to confinement/deconfinement phase transition at finite temperature [26, 27]. The holographic entanglement entropy becomes an effective tool for testing phase transitions in CFT. Note that purely classical gravity calculations provide an insight to non-trivial quantum properties of the corresponding field theories.

ACKNOWLEDGMENTS

P. K. was supported by Grant GAČR P203/12/0118 and appreciates the hospitality of the TPI of the University of Alberta. A. Z. thanks the Natural Sciences and Engineering Research Council of Canada and the Killam Trust for financial support and appreciates the hospitality of the ITP MFF of the Charles University in Prague.

[1] J. Bekenstein, Lett. Nuovo Cim. **4**, 737 (1972).
[2] S. Hawking, Commun. Math. Phys. **25**, 152 (1972).
[3] L. Bombelli, R. K. Koul, J. Lee, and R. D. Sorkin, Phys. Rev. D **34**, 373 (1986).
[4] M. Srednicki, Phys. Rev. Lett. **71**, 666 (1993), arXiv:hep-th/9303048 [hep-th].
[5] A. Barvinsky, V. P. Frolov, and A. Zelnikov, Phys. Rev. D **51**, 1741 (1995), arXiv:gr-qc/9404036 [gr-qc].
[6] L. Susskind and J. Uglum, Phys. Rev. D **50**, 2700 (1994), arXiv:hep-th/9401070 [hep-th].
[7] A. Sakharov, Sov. Phys. Dokl. **12**, 1040 (1968).
[8] T. Jacobson, (1994), preprint, arXiv:gr-qc/9404039 [gr-qc].
[9] V. P. Frolov, D. Fursaev, and A. Zelnikov, Nucl. Phys. **B486**, 339 (1997), arXiv:hep-th/9607104 [hep-th].
[10] V. P. Frolov, D. Fursaev, and A. Zelnikov, Nucl. Phys. Proc. Suppl. **57**, 192 (1997).
[11] V. P. Frolov, D. Fursaev, and A. Zelnikov, JHEP **0303**, 038 (2003), arXiv:hep-th/0302207 [hep-th].
[12] S. Ryu and T. Takayanagi, Phys. Rev. Lett. **96**, 181602 (2006), arXiv:hep-th/0603001 [hep-th].
[13] S. Ryu and T. Takayanagi, JHEP **0608**, 045 (2006), arXiv:hep-th/0605073 [hep-th].
[14] T. Nishioka, S. Ryu, and T. Takayanagi, J. Phys. **A42**, 504008 (2009), arXiv:0905.0932 [hep-th].
[15] D. V. Fursaev, JHEP **0609**, 018 (2006), arXiv:hep-th/0606184 [hep-th].
[16] T. Hartman, (2013), preprint, arXiv:1303.6955 [hep-th].
[17] T. Faulkner, (2013), preprint, arXiv:1303.7221 [hep-th].
[18] A. Lewkowycz and J. Maldacena, JHEP **1308**, 090 (2013), arXiv:1304.4926 [hep-th].
[19] T. Faulkner, A. Lewkowycz, and J. Maldacena, (2013), preprint, arXiv:1307.2892 [hep-th].
[20] L.-Y. Hung, R. C. Myers, and M. Smolkin, JHEP **1104**, 025 (2011), arXiv:1101.5813 [hep-th].
[21] H. Casini, M. Huerta, and R. C. Myers, JHEP **1105**, 036 (2011), arXiv:1102.0440 [hep-th].
[22] R. C. Myers, R. Pourhasan, and M. Smolkin, JHEP **1306**, 013 (2013), arXiv:1304.2030 [hep-th].
[23] A. Bhattacharyya, A. Kaviraj, and A. Sinha, JHEP **1308**, 012 (2013), arXiv:1305.6694 [hep-th].
[24] L.-Y. Hung, R. C. Myers, and M. Smolkin, JHEP **1108**, 039 (2011), arXiv:1105.6055 [hep-th].
[25] S. N. Solodukhin, Living Rev. Rel. **14**, 8 (2011), arXiv:1104.3712 [hep-th].
[26] I. R. Klebanov, D. Kutasov, and A. Murugan, Nucl. Phys. **B796**, 274 (2008), arXiv:0709.2140 [hep-th].
[27] A. Lewkowycz, JHEP **1205**, 032 (2012), arXiv:1204.0588 [hep-th].
[28] T. Hirata and T. Takayanagi, JHEP **0702**, 042 (2007), arXiv:hep-th/0608213 [hep-th].
[29] M. Headrick and T. Takayanagi, Phys. Rev. D **76**, 106013 (2007), arXiv:0704.3719 [hep-th].
[30] V. E. Hubeny and M. Rangamani, JHEP **0803**, 006 (2008), arXiv:0711.4118 [hep-th].
[31] P. Krtouš and A. Zelnikov, "Minimal surfaces and entanglement entropy in anti-de Sitter space," unpublished, in preparation.
[32] R. C. Myers and A. Sinha, JHEP **1101**, 125 (2011), arXiv:1011.5819 [hep-th].
[33] T. Takayanagi, Class. Quant. Grav. **29**, 153001 (2012), arXiv:1204.2450 [gr-qc].
[34] I. S. Gradshtein and I. M. Ryzhik, *Table of Integrals, Series, and Products* (Academic Press, New York, 1994).
[35] E. Tonni, JHEP **1105**, 004 (2011), arXiv:1011.0166 [hep-th].